The Rab27a effector exophilin7 promotes fusion of secretory granules that have not been docked to the plasma membrane

Hao Wang*, Ray Ishizaki*, Jun Xu*, Kazuo Kasai, Eri Kobayashi, Hiroshi Gomi, and Tetsuro Izumi
Department of Molecular Medicine, Institute for Molecular and Cellular Regulation, Gunma University, Maebashi 371-8512, Japan

ABSTRACT **Granuphilin, an effector of the small GTPase Rab27a, mediates the stable attachment (docking) of insulin granules to the plasma membrane and inhibits subsequent fusion of docked granules, possibly through interaction with a fusion-inhibitory Munc18-1/syntaxin complex. However, phenotypes of insulin exocytosis differ considerably between Rab27a- and granuphilin-deficient pancreatic β cells, suggesting that other Rab27a effectors function in those cells. We found that one of the putative Rab27a effector family proteins, exophilin7/JFC1/Slp1, is expressed in β cells; however, unlike granuphilin, exophilin7 overexpressed in the β-cell line MIN6 failed to show granule-docking or fusion-inhibitory activity. Furthermore, exophilin7 has no affinities to either Munc18-1 or Munc18-1–interacting syntaxin-1a, in contrast to granuphilin. Although β cells of exophilin7-knockout mice show no apparent abnormalities in intracellular distribution or in ordinary glucose-induced exocytosis of insulin granules, they do show impaired fusion in response to some stronger stimuli, specifically from granules that have not been docked to the plasma membrane. Exophilin7 appears to mediate the fusion of undocked granules through the affinity of its C2A domain toward the plasma membrane phospholipids. These findings indicate that the two Rab27a effectors, granuphilin and exophilin7, differentially regulate the exocytosis of either stably or minimally docked granules, respectively.**

Monitoring Editor
Thomas F. J. Martin
University of Wisconsin

Received: Apr 5, 2012
Revised: Nov 21, 2012
Accepted: Nov 26, 2012

INTRODUCTION

The small GTPase Rab27a and its isoform, Rab27b, are specifically expressed in a wide range of exocytic cells (Tolmachova *et al.*, 2004; Gomi *et al.*, 2007) and regulate exocytosis of secretory vesicles through the family of their effectors called exophilins or Slp/Slac, which share an N-terminal homologous Rab27-binding region (Izumi *et al.*, 2003; Fukuda, 2005). For example, in pancreatic endocrine cells, Rab27a and its effectors, granuphilin and exophilin4, form a complex on secretory granules and regulate insulin and glucagon secretion, respectively (Torii *et al.*, 2002, 2004; Yi *et al.*, 2002; Yu *et al.*, 2007). However, analyses of pancreatic β cells derived from mutant mice demonstrated that, whereas granuphilin is indispensable for the docking of insulin granules to the plasma membrane and simultaneously inhibits insulin exocytosis, Rab27a seems to be dispensable for granule docking but positively regulates exocytosis through granule recruitment near the plasma membrane (Gomi *et al.*, 2005; Kasai *et al.*, 2005, 2008). These differential phenotypes suggest that Rab27a mediates insulin exocytosis not only through granuphilin, but also through other effectors expressed in pancreatic β cells. Indeed, several candidate Rab27a effectors, such as exophilin8/MyRIP/Slac2-c and Noc2, have been reported to be expressed and function in pancreatic β cells (Waselle *et al.*, 2003; Matsumoto *et al.*, 2004; Mizuno *et al.*, 2011). However, the function of those effectors has not been fully investigated to account for the phenotype of Rab27a-mutated β cells.

In screening the candidate Rab27a effectors expressed in pancreatic β cells in the present study, we found that exophilin7, also

This article was published online ahead of print in MBoC in Press (http://www.molbiolcell.org/cgi/doi/10.1091/mbc.E12-04-0265) on December 5, 2012.

*These authors contributed equally to this work.

Address correspondence to: Tetsuro Izumi (tizumi@gunma-u.ac.jp).

Abbreviations used: β-gal, β-galactosidase; EGFP, enhanced green fluorescent protein; GST, glutathione *S*-transferase; HA, hemagglutinin; PI, phosphoinositide; PIP_2, phosphatidylinositol 4,5-bisphosphate; PIP_3, phosphatidylinositol 3,4,5-triphosphate; PKC, protein kinase C; PMA, phorbol-12-myristate-13-acetate; PS, phosphatidylserine; TIRF, total internal reflection fluorescence.

known as JFC1 or Slp1, is located on insulin granules. It was previously reported that the modulation of an exophilin7 expression level affects exocytosis in complex manners. The overexpression of exophilin7 significantly increases the secretion of prostate-specific antigen, but not of prostatic-specific acid phosphatase, in LNCap prostate carcinoma cells (Johnson *et al.*, 2005). Furthermore, the small interfering RNA–mediated down-regulation of exophilin7 causes impaired myeloperoxidase secretion in the promyelocytic leukemia cell line HL-60 (Brzezinska *et al.*, 2008), whereas pancreatic acinar cells isolated from exophilin7-null mice in a fasting but not in a fed state exhibit increases in the number of zymogen granules and in amylase secretion in response to strong stimuli (Saegusa *et al.*, 2008). Because it is unknown which secretory process is impaired, the function of exophilin7 remains elusive. In the present study, we found that exophilin7 overexpressed in the β-cell line MIN6 neither promotes granule targeting to the plasma membrane nor inhibits granule fusion, in contrast to granuphilin. However, exophilin7-deficient β cells did show impairment of a specific type of exocytosis, in which granules fuse without stable attachment to the plasma membrane. Therefore, despite their close resemblance in domain structure and tissue distribution, granuphilin and exophilin7 differentially mediate the exocytosis in a parallel way, mediating either stably or minimally docked granules, respectively. A biochemical characterization of the interacting molecules suggested that, whereas the protein interaction with Munc18-1 and/or Munc18-1–interacting syntaxin is critical for granuphilin to function on docked granules, the affinity to phospholipids on the plasma membrane is essential for exophilin7 to promote exocytosis of undocked granules.

RESULTS

Exophilin7 is expressed in pancreatic islets

Exophilin7 cDNA was amplified from the cDNA of the pancreatic β-cell line MIN6. Polyclonal antibody generated against the N-terminus of exophilin7 detected three proteins whose molecular masses were ~57–76 kDa in the extract of pancreatic islets (Figure 1A). Because the N-terminal Rab27-binding regions are shared among the Rab27 effector family proteins (Izumi *et al.*, 2003; Fukuda, 2005), it is possible that the antibody raised against the protein containing this region recognizes other Rab27 effectors. Indeed, the upper, 76-kDa protein and the lower, 57-kDa protein appeared to be two granuphilin isoforms—granuphilin-a and -b, respectively (Wang *et al.*, 1999)—because these two protein bands disappeared in the islet extract of granuphilin-null mice (Gomi *et al.*, 2005). By contrast, the middle, 63-kDa protein disappeared in the extracts of newly made exophilin7-knockout mice (see discussion of Figure 3), indicating that it corresponds to exophilin7, whose calculated molecular mass is 62,358 Da. All three proteins disappeared in the extracts of granuphilin/exophilin7 double-knockout mice (see discussion of Figure 6) and formed an endogenous complex with Rab27a (Supplemental Figure S1). Thus our anti-exophilin7 antibody recognizes both exophilin7 and granuphilin. An analysis of tissue distribution revealed that exophilin7 was specifically expressed in pituitary, pancreatic islets, and the β-cell line MIN6 but not in other major tissues, such as liver tissue or the α-cell line αTC1.6 (Figure 1B), which was remarkably similar to the distribution of granuphilin (Wang *et al.*, 1999).

Exophilin7 is localized on insulin granules but apparently has no effect on their distribution or exocytosis in MIN6 cells

We then investigated intracellular localization of exophilin7 in MIN6 cells. Because our anti-exophilin7 antibody also recognizes granuphilin, we examined the intracellular localization of hemagglutinin (HA)-tagged exophilin7 exogenously expressed in MIN6 cells. Double-immunostaining analyses indicated that HA-exophilin7 was partially colocalized with insulin (Figure 2A; see also discussion of Supplemental Figure S4). Quantification revealed that 56.3 ± 4.2% (n = 21) of all HA-exophilin7–positive puncta contain insulin, suggesting that 43.7% of HA-exophilin7 locate on other unknown vesicles. On the other hand, 41.2 ± 3.6% (n = 21) of insulin-positive puncta contain HA-exophilin7, indicating that 58.8% of insulin granules do not harbor exophilin7 but may harbor no or other Rab27a effectors such as granuphilin. Biochemical subcellular fractionation of MIN6 cellular membranes in a linear sucrose density gradient also indicated that endogenous exophilin7 was cofractionated with insulin granules (Figure 2B). There were slight shifts among the peaks of distributions of insulin, Rab27a, and its effectors exophilin7 and granuphilin, which may reflect that Rab27a and its effectors are sequentially associated on a certain mature stage of insulin granules, as was reported for Rab27a on endothelial Weibel–Palade bodies (Hannah *et al.*, 2003).

We previously established a stable MIN6 cell line that expressed a phogrin–enhanced green fluorescent protein (EGFP) fusion protein as a fluorescent marker of insulin granules and showed that overexpression of granuphilin promotes the plasma membrane targeting of insulin granules (Torii *et al.*, 2004). In the present study, we infected those MIN6 cells with recombinant adenovirus encoding either HA-exophilin7 or HA-granuphilin cDNA. Under the condition that the MIN6 cells expressed a similar level of exogenous exophilin7 or granuphilin, we examined changes in the granule distribution by tracking the EGFP fluorescence (Figure 2C). As shown previously, cells that expressed granuphilin exhibited a prominent peripheral redistribution of labeled granules along the plasma membrane compared with those expressing control β-galactosidase (β-gal) protein. By contrast, cells that expressed exophilin7 did not display such a peripheral redistribution of granules. Quantitative measurement revealed that exophilin7 has essentially no granule-targeting activity (Figure 2D). We then examined the effect of overexpressed exophilin7 on insulin exocytosis. Although overexpression of granuphilin

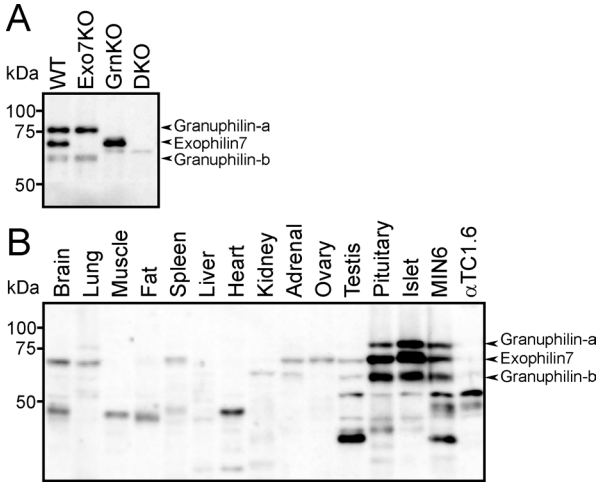

FIGURE 1: Exophilin7 is specifically expressed in pancreatic islets. (A) The total islet protein lysates (5 μg) from wild-type (WT), exophilin7-knockout (Exo7KO), granuphilin-knockout (GrnKO), or exophilin7/granuphilin double-knockout (DKO) mice were analyzed by immunoblotting with anti-exophilin7 antibody. (B) An equal amount of protein (10 μg) from tissue and cell extracts was analyzed by immunoblotting with anti-exophilin7 antibody.

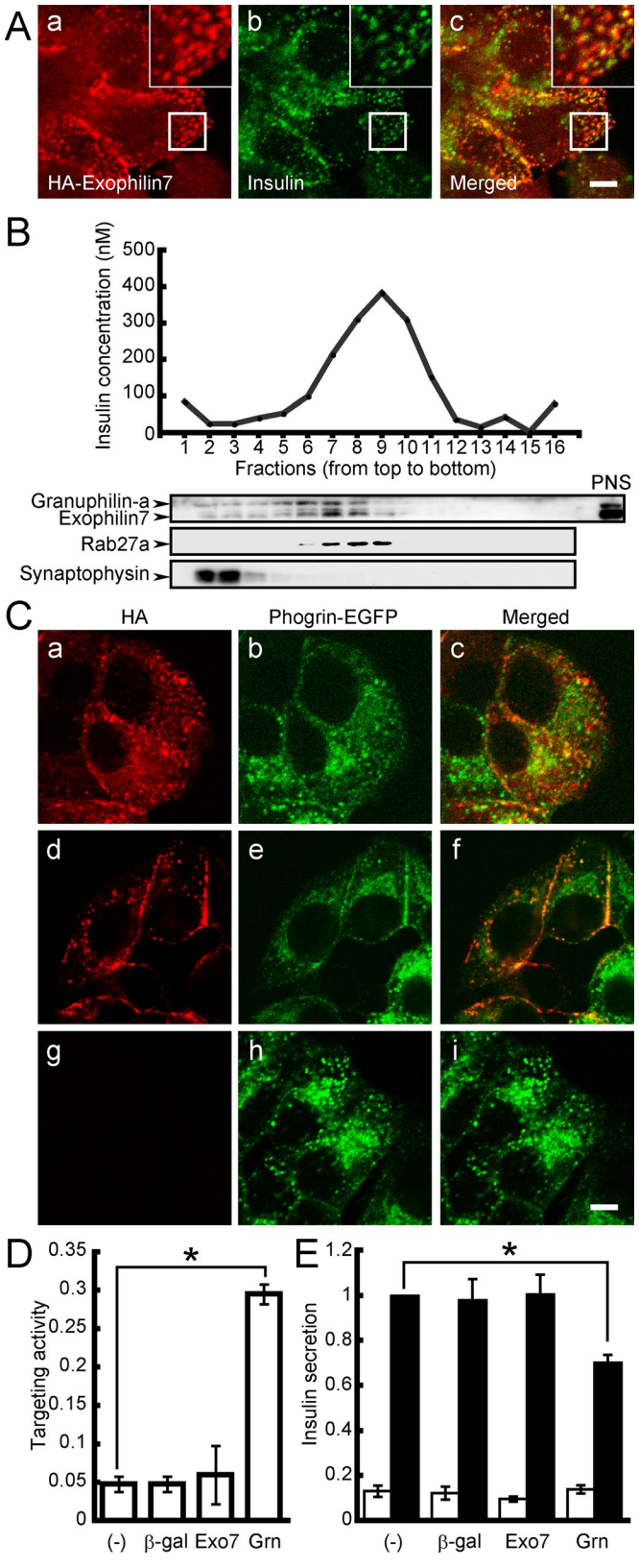

FIGURE 2: Exophilin7 is localized on insulin granules but shows inert exocytic activities in MIN6 cells. (A) MIN6 cells were infected with recombinant adenovirus encoding HA-tagged exophilin7 cDNA. They were then double immunostained with monoclonal anti-HA and polyclonal anti-insulin antibodies and observed with a confocal laser-scanning microscope. Merged fluorescence signals are also shown. Details are shown at a higher magnification (insets). Bar, 5 μm. (B) The crude organelle fraction prepared from a postnuclear supernatant (PNS) of MIN6 cells was separated on a linear sucrose density gradient. Sixteen fractions were collected, and immunoreactive insulin in a portion of each fraction was measured (top). Equal volumes of the fractions were analyzed by immunoblotting using antibodies against exophilin7, Rab27a, and the marker of synaptic-like microvesicles synaptophysin. (C) MIN6 cells that stably expressed phogrin-EGFP were infected with recombinant adenovirus encoding HA-tagged exophilin7 (a–c), granuphilin-a (d–f), or control β-gal (g–i) cDNA, and the plasma membrane targeting of fluorescently labeled granules was examined. The anti-HA immunostaining (a, d, and g) and intrinsic EGFP signals (b, e, and h) were observed with a confocal microscope. Merged fluorescence signals are also shown (c, f, and i). Bar, 5 μm. (D) The granule-targeting activities of exophilin7 (Exo7) and granuphilin (Grn) were analyzed semiquantitatively in all cells in six pictures (bottom). The total numbers of cells analyzed were 178, 217, 178, and 285 for noninfected cells or those infected with adenoviruses encoding β-gal, HA-exophilin7, and HA-granuphilin-a cDNA, respectively. Values are means ± SEM ($n = 3$). (E) Noninfected MIN6 cells or those infected with adenoviruses encoding β-gal, HA-Exo7, or HA-Grn cDNA were incubated for 2 h in standard low-glucose (2.8 mM) Krebs–Ringer buffer. The cells were then incubated for 30 min in the buffer (open bars) or that containing 60 mM KCl–65 mM NaCl (closed bars). Values were normalized to the release of insulin from uninfected MIN6 cells stimulated by high potassium. The results are given as means ± SEM ($n = 6$). The statistical significance was assessed by analysis of variance (Tukey–Kramer method; $^*p < 0.0001$ vs. uninfected cells).

significantly decreased high potassium-induced insulin secretion as reported previously (Torii *et al.*, 2002), that of exophilin7 had no such effect (Figure 2E). Thus overexpression of exophilin7 affects neither granule distribution nor exocytosis.

Exophilin7-null mice do not show overt glucose intolerance

Although exophilin7 overexpression in MIN6 cells does not affect insulin granule location or exocytosis, its down-regulation might reveal other aspects of its function. For this purpose, we generated a mouse line lacking exophilin7 using the gene-knockout approach (Figure 3, A and B). Exophilin7-null mice showed normal development and were fertile, with no apparent abnormalities in general appearance or behavior. Immunoblot analysis confirmed the absence of exophilin7, but not that of granuphilin, in the isolated islet extracts of exohilin7-null mice (Figure 3C). The expression levels of Rab27a and granuphilin-interacting syntaxin-1a or Munc18-1 were not altered in the exophilin7-deficient islets compared with the wild-type controls. We then examined in vivo phenotypes that might be affected by potential insulin secretion defects. The male mice showed normal body weight (Figure 3D) and no significant changes in the blood glucose (Figure 3E) or serum insulin (Figure 3F) levels examined in fasting mice or after a glucose load, although they tended to exhibit increased glucose levels and decreased insulin levels compared with those of wild-type mice. An insulin tolerance test showed comparable insulin sensitivity between the mutant and control mice (Figure 3G). These findings indicate that exophilin7-null mice exhibit no gross alterations in glucose tolerance or insulin secretion at the body level.

Exophilin7-null islets exhibit decreased insulin secretion in response to high potassium-induced depolarization and to protein kinase C activation

We then performed an electron microscopic analysis of exophilin7-null β cells to examine the intracellular distribution of the insulin

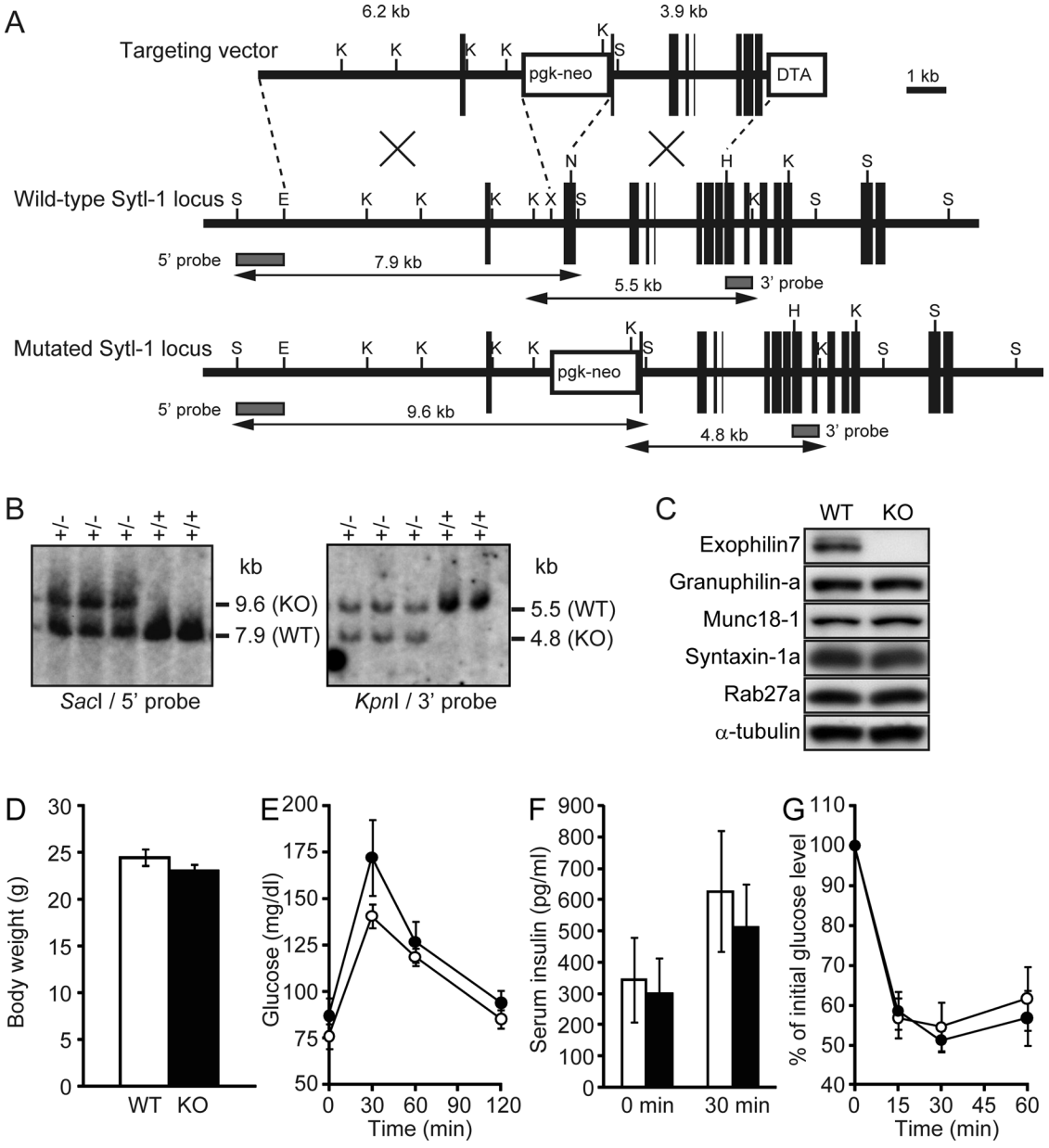

FIGURE 3: Exophilin7-deficient mice show normal glucose tolerance. (A) Targeted disruption of the exophilin7 gene (*Sytl-1*) on mouse chromosome 4 by insertion of *pgk-neo*. The targeting vector contains a neomycin resistance gene driven by the *pgk* promoter (pgk-neo) and a diphtheria toxin A–fragment (DTA) gene driven by the *MC1* promoter as positive and negative selection markers, respectively. Exon structures are vertically lined and shown from exon 1 to exon 15. Homologous recombination results in replacement of the genomic region from exon 2 with *pgk-neo*. (B) Genomic Southern hybridization analysis of the neomycin-resistant embryonic stem cell clones. The locations of the 5′ and the 3′ external probes are shown with horizontal closed boxes in A. The 5′ probe hybridizes to *Sac*I fragments of 7.9 and 9.6 kb from wild-type (WT) and mutant knockout (KO) alleles, respectively. Similarly, the 3′ probe hybridizes to *Kpn*I fragments of 5.5 and 4.8 kb from the WT and KO alleles, respectively. (C) An equal amount of protein (5 μg) from the islets of WT and KO mice was electrophoresed for immunoblotting with antibodies toward the indicated proteins. (D–G) In vivo phenotypes of exophilin7-KO mice. Each measurement was performed in age-matched (9- to 16-wk-old) WT (open bars and circles, $n = 7$) and KO (closed bars and circles, $n = 7$) male mice. (D) Body weight. (E) Blood glucose concentrations during an intraperitoneal glucose tolerance test. (F) Serum insulin concentrations before and 30 min after a glucose load. (G) Percentage of starting blood glucose concentration during an intraperitoneal insulin tolerance test. Results are presented as means ± SEM. The statistical significance of differences between means was assessed by a repeated measure of analysis of variance (Tukey–Kramer method).

granules (Figure 4A). The average granule number per cytosol area (μm^2) was not significantly different between exophilin7-null (3.08 ± 0.15) and wild-type β cells (2.76 ± 0.15). When all insulin granules located in a single section were categorized according to their distance from the granule center to the plasma membrane, the relative number of granules in each bin did not differ between the mutant and control β cells (Figure 4B). Furthermore, there was no change in the number of granules having centers residing <200 nm from the

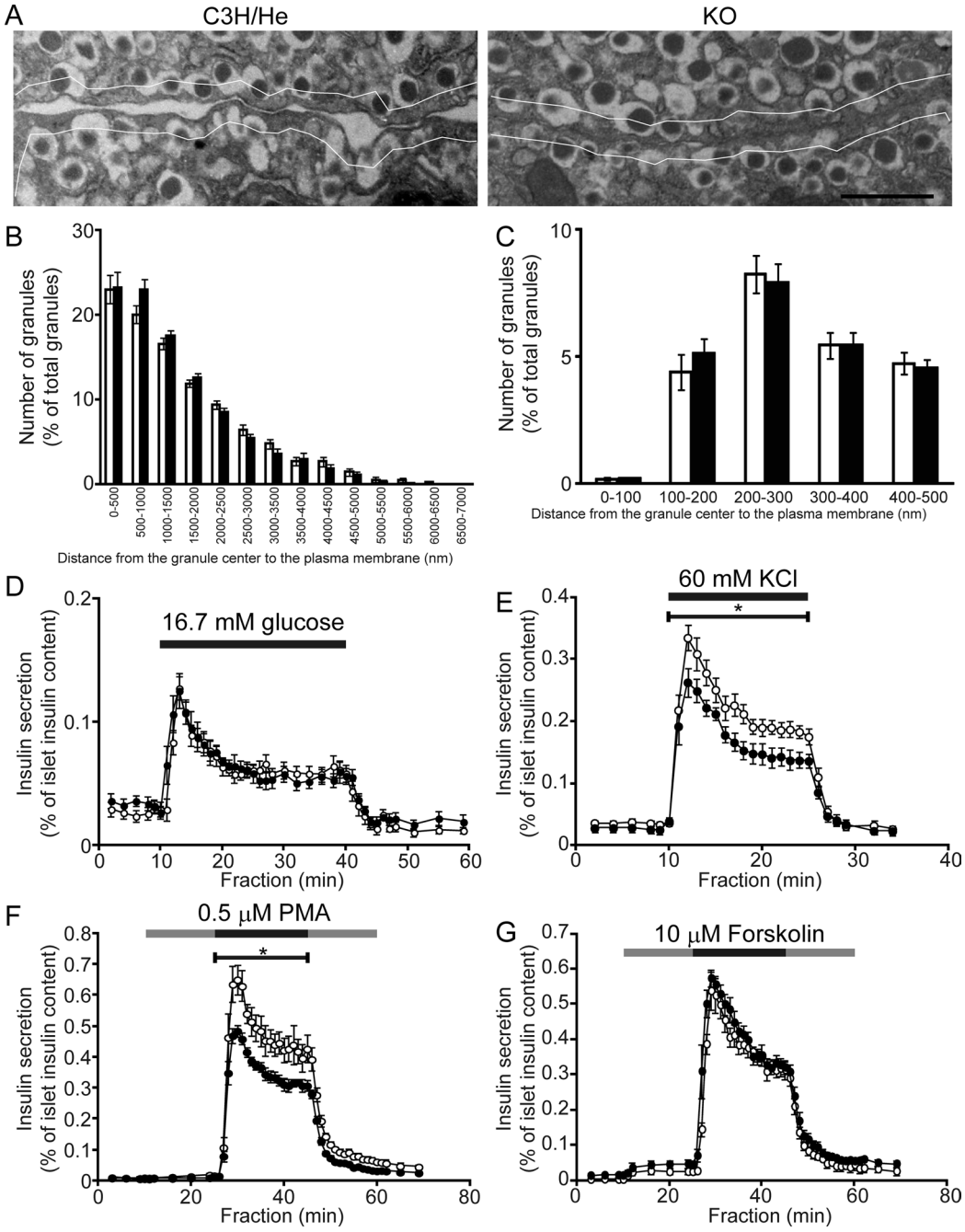

FIGURE 4: Electron microscopic analysis and insulin secretion profiles in isolated islets. (A) Isolated islets cultured overnight were incubated in 2.8 mM glucose buffer at 37°C for 1 h. They were then fixed and processed in a standard manner for electron microscopy. Electron micrographs of β cells from C3H/He and exophilin7-knockout (KO) mice are shown. Solid lines indicate a 200-nm distance from the plasma membrane. Bar, 1 μm. (B, C) The distributions of insulin granules were morphometrically analyzed in β cells of 24- to 28-wk-old male wild-type (open columns, $n = 3$) and exophilin7-knockout (closed columns, $n = 3$) mice. All granules (B) and those with centers that resided within 500 nm of the plasma membrane (C) were categorized at 500- and 100-nm intervals, respectively. Data are shown as a percentage of the total granule number (means ± SEM; $n = 9$). (D–G) Islets isolated from age-matched (20- to 30-wk-old) male wild-type (open circles, $n = 8$ for D, $n = 10$ for E, $n = 5$ for F and G) or exophilin7-knockout (closed circles, $n = 6$ for D, $n = 8$ for E, $n = 5$ for F and G) mice were perifused with standard low-glucose (2.8 mM) Krebs–Ringer buffer for 30 min. Thereafter the collection of each fraction (1 ml/min) was started, and an appropriate secretagogue was applied at 10 min after the start. (D) Islets were perifused with the buffer containing 16.7 mM glucose for 30 min (horizontal black line), followed by that containing 2.8 mM glucose for 20 min. (E) Islets were perifused with the buffer containing 60 mM KCl for 15 min, followed by the standard buffer for 10 min. (F, G) In the continuous presence (black and gray lines) of either 0.5 μM PMA (F) or 10 μM forskolin (G), islets were stimulated by 16.7 mM glucose buffer for 20 min (black line), with preincubation and postincubation stimulation of 2.8 mM glucose buffer for 15 min (gray line). All results are presented as the mean ± SEM. The statistical significance of differences between means or the areas under the curve was assessed by a Mann–Whitney *U* test. *$p < 0.05$.

plasma membrane (Figure 4C), which should comprise nearly all the docked granules, given that the diameter of insulin granules is ~350 nm (Gomi *et al.*, 2005). These findings indicate that exophilin7 has no effect on the intracellular distribution or plasma membrane–docking of insulin granules.

We next assessed the insulin-secretory ability of isolated islets by perifusion analyses. Consistent with their almost normal glucose tolerance (Figure 3E), exophilin7-null islets showed no significant change in either the early or late phase of insulin secretion in response to 16.7 mM glucose (Figure 4D). However, they did show a significantly decreased insulin secretory response to depolarization by 60 mM KCl (Figure 4E; $p < 0.05$). The amplitude and time course of the depolarization-induced rise of the cytoplasmic Ca^{2+} concentration were similar between pancreatic β cells isolated from C3H/He and exophilin7-knockout mice (Supplemental Figure S2). It should be noted that this stimulation induced much higher insulin secretion compared with the 16.7 mM glucose stimulation. Stimulation by phorbol-12-myristate-13-acetate (PMA; a protein kinase C [PKC] activator) in the presence of 16.7 mM glucose induced yet higher secretion, even compared with the 60 mM KCl stimulation, and revealed a significantly decreased secretory response in exophilin7-null islets (Figure 4F; $p < 0.05$). Of interest, the effect of forskolin (an activator of adenylate cyclase) in the presence of 16.7 mM glucose was indistinguishable between the mutant and control islets, although individual stimulation by forskolin or PMA induced a comparable level of insulin secretion (Figure 4G). The differential effects of each secretagogue likely reflect differences in the mode of granule recruitment or priming for fusion. Overall, exophilin7-null islets showed significantly lower insulin secretion in response to at least two kinds of strong stimuli: potassium-induced depolarization and PKC activation.

Exophilin7 promotes exocytosis of undocked granules

Time-lapse imaging recordings under total internal reflection fluorescence (TIRF) microscopy in living cells permit direct observation of the fusion events of secretory granules, as well as analysis of the prefusion behavior of fused granules. Previous TIRF microscopic analyses in pancreatic β cells indicated that insulin granules are not uniformly processed prior to their fusion (Ohara-Imaizumi *et al.*, 2004; Shibasaki *et al.*, 2007; Kasai *et al.*, 2008). For example, in our study of mouse pancreatic β cells expressing EGFP-fused human insulin (Kasai *et al.*, 2008), fused insulin granules were categorized into three classes depending on the prefused behavior: the granule visible before stimulation, *residents*; those that have become visible during the stimulation, *visitors*; and those without stable visualization before fusion, *passengers* (Supplemental Figure S3). We compared the exocytic profiles of insulin granules between β cells of wild-type and exophilin7-null mice in response to high potassium stimulation (60 mM KCl, 5 min), which induced significantly different insulin-secretory responses between islets of those two mice (Figure 4E). As previously reported (Kasai *et al.*, 2008), fusion events in response to this depolarization stimulus mostly occurred within the first 1 or 2 min and involved previously visible *residents* in wild-type β cells (Figure 5A and Supplemental Video S1). Although a roughly similar exocytic profile was seen in exophilin7-null β cells (Figure 5B and Supplemental Video S2), quantitative comparison revealed that the number of fusion events from *passengers* is decreased ($p < 0.05$; Figure 5C). These findings suggest that exophilin7 is involved in the exocytosis of at least a *passenger* type of granule, which shows no stable attachment (docking) to, or significant stalling near, the plasma membrane before fusion (Kasai *et al.*, 2008).

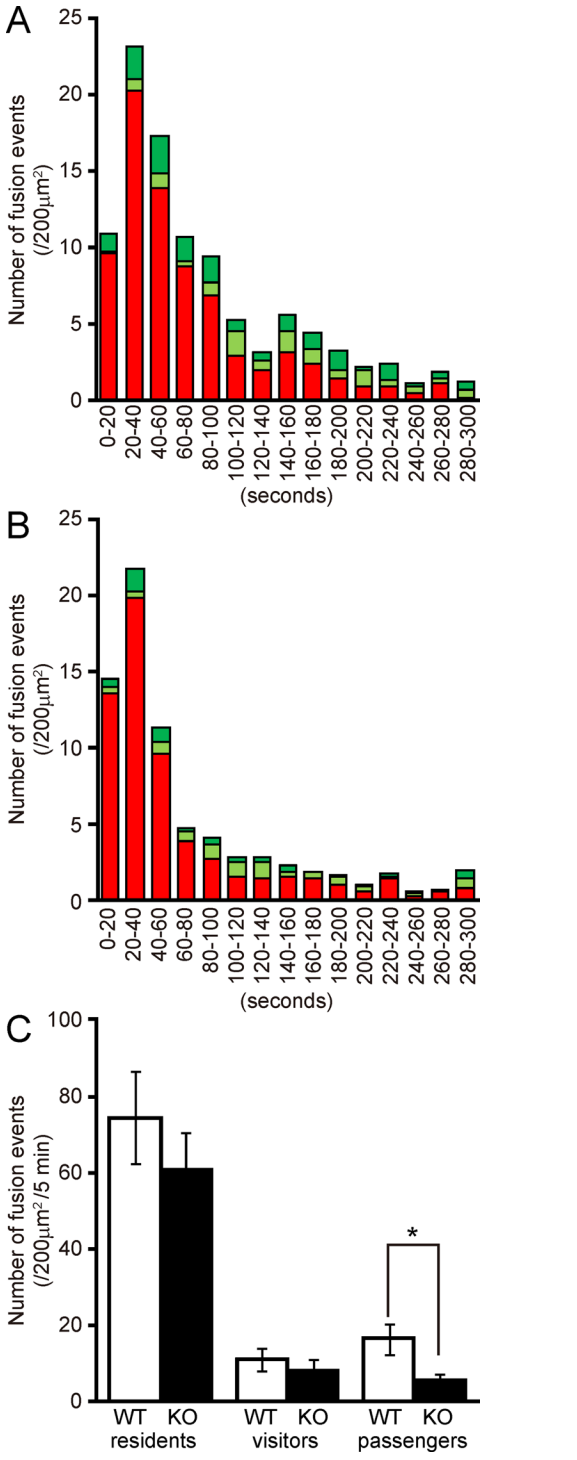

FIGURE 5: TIRF microscopic analysis of high potassium–induced exocytosis. (A, B) TIRF microscopic images were sampled every 101.7 ms in living β cells expressing EGFP-labeled insulin from wild-type (WT; A) or exophilin7-knockout (KO; B) mice. All fusion events after high-potassium stimulation (60 mM KCl, 5 min) were manually counted in each cell ($n = 10$). Time 0 indicates the initiation of stimulation. The histograms show the number of fusion events per 200 μm² at 20-s intervals from *residents* (red), *visitors* (light green), and *passengers* (deep green), respectively. (C) The number of fusion events during the stimulation is summed for each category of granules in WT (open columns) and KO (closed columns) cells. Data are expressed as the mean ± SEM. The statistical significance of differences between means was assessed by a Mann–Whitney *U* test. *$p < 0.05$.

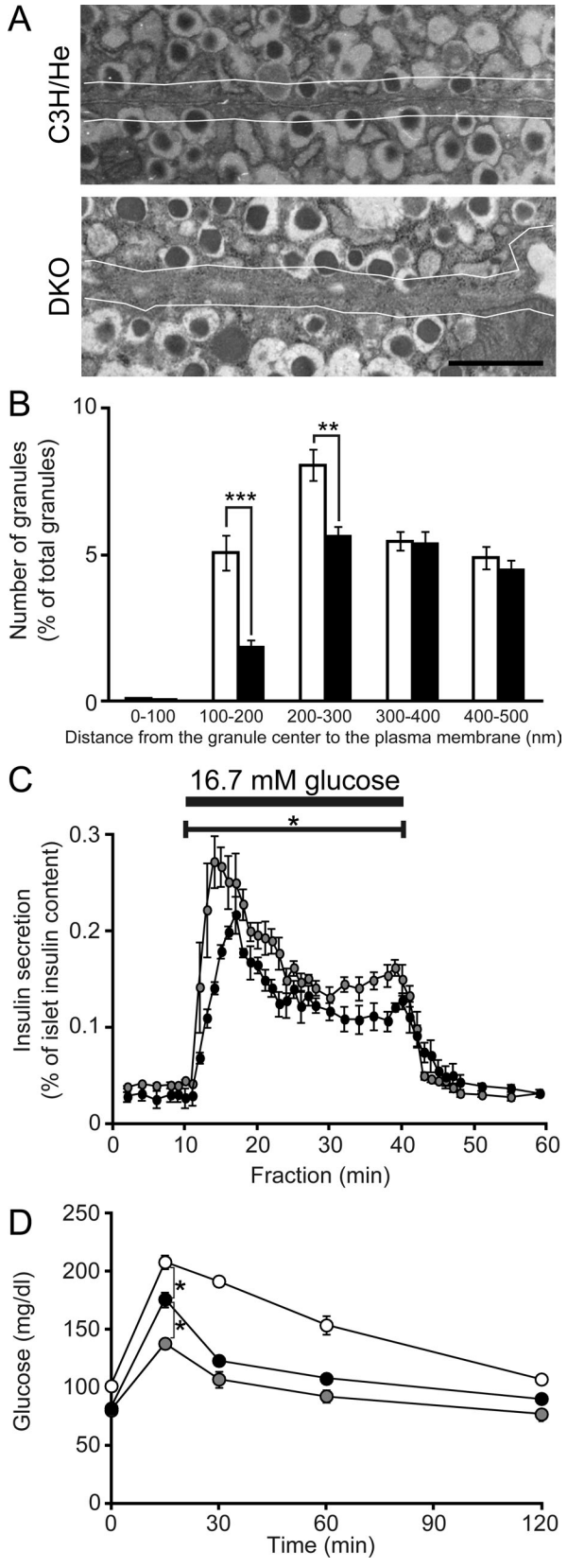

FIGURE 6: Granuphilin/exophilin7 double-knockout mice show decreased insulin secretion and glucose tolerance. (A) Electron micrographs of β cells from C3H/He and granuphilin/exophilin7 double-knockout (DKO) mice. Solid lines indicate a 200-nm distance from the plasma membrane. Bar, 1 μm. (B) Insulin granules with centers residing within 500 nm of the plasma membrane in β cells from 24- to 28-wk-old male C3H/He (white columns, $n = 3$) and DKO (black columns, $n = 3$) mice were categorized into five bins. (C) Islets isolated from age-matched (20- to 30-wk-old) male granuphilin-knockout (gray circles, $n = 4$) or double-knockout (black circles, $n = 4$) mice were perifused with the buffer containing 16.7 mM glucose for 30 min (horizontal black line), followed by 2.8 mM glucose buffer for 20 min. (D) Blood glucose concentrations during an intraperitoneal glucose tolerance test in 20-wk-old male wild-type (white circles; $n = 4$), granuphilin-knockout (gray circles; $n = 4$), and double-knockout (black circles; $n = 4$) mice. The statistical significance of differences between means was assessed by a Mann–Whitney *U* test (B, C) or analysis of variance (Tukey–Kramer method; D). *$p < 0.05$; **$p < 0.005$; ***$p < 0.001$.

Exophilin7 deficiency affects glucose-induced insulin secretion in the absence of granuphilin

The apparently specific effects on fusion of undocked granules in exophilin7-null β cells prompted us to investigate the effects of exophilin7 deficiency in the absence of granuphilin, in which stably docked granules are lost and total exocytosis from undocked granules is enhanced (Gomi *et al.*, 2005). For this purpose, we generated double-mutant mice by crossing exophilin7-knockout mice with granuphilin-knockout mice. The double-mutant mice were viable and showed no gross abnormalities in development or behavior, as in the individually mutated mice. We confirmed by electron microscopy that docked granules whose limiting membrane was directly attached to the plasma membrane were missing in the double-mutant β cells (Figure 6A), as was found in granuphilin-null β cells (Gomi *et al.*, 2005). Morphometrical analysis revealed that the number of granules with centers that resided within 300 nm of the plasma membrane was specifically decreased (Figure 6B). We then examined evoked insulin secretion in perifused islets of the double-mutant mice. Previous findings using mutant mice indicated that Rab27a has a positive effect on glucose-induced insulin secretion (Kasai *et al.*, 2005), whereas granuphilin has a negative effect on it (Gomi *et al.*, 2005). If exophilin7 is inert for exocytosis and only passively promotes exocytosis by competitively inhibiting Rab27a from forming a complex with secretion-inhibitory granuphilin, any effect of exophilin7 deficiency should be canceled by the absence of granuphilin. By contrast, if exophilin7 is actively involved in evoked exocytosis of undocked granules independent of the presence of granuphilin, the effect of exophilin7 deficiency may be more overt when exocytosis of undocked granules is enhanced in the absence of granuphilin. Although exophilin7 deficiency had no effect on glucose-induced insulin secretion in the presence of granuphilin (Figure 4D), it caused a significantly greater inhibitory effect on it in the absence of granuphilin (Figure 6C; $p < 0.05$). Consistently, blood glucose levels examined at 15 min after a glucose load in the double-mutant mice (Figure 6D) were significantly higher than those in the granuphilin-null mice ($p < 0.05$), although they were still lower than those in the wild-type mice because of the granuphilin deficiency ($p < 0.05$). These findings indicate that exophilin7 is not a mere buffer to prevent Rab27a from binding with granuphilin but also plays an active role in promoting the fusion of undocked granules. Thus granuphilin and exophilin7, the two Rab27a effectors coexpressed in β cells, play differential roles in the exocytosis of docked and undocked granules, respectively.

Exophilin7 has no affinity to Munc18-1 or syntaxin-1a

The marked differences in the exocytic activities between the two Rab27a effectors prompted us to compare their biochemical characteristics. Granuphilin is believed to mediate granule docking through

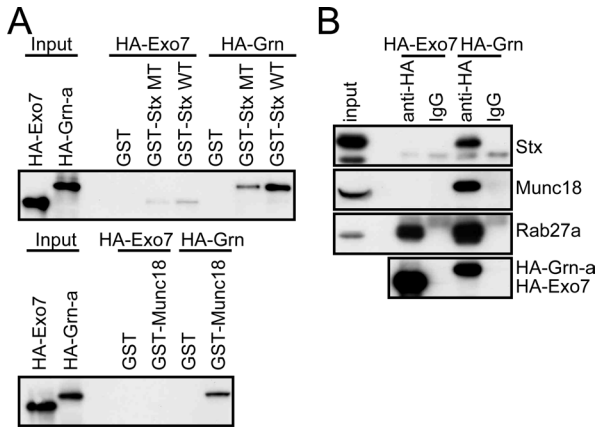

FIGURE 7: Exophilin7 has no affinity to Munc18-1 or syntaxin-1a. (A) GST-fused wild-type (WT) or L165A/E166A mutant (MT) rat syntaxin-1a (Stx; top), GST-fused mouse Munc18-1 (Munc18; bottom), or control GST protein immobilized to glutathione beads (10 μg each) were incubated with in vitro–translated, HA-tagged exophilin7 (Exo7) or granuphilin (Grn)-a. Bound proteins, as well as 1/20 of the in vitro–translated products, were analyzed by immunoblotting with anti-HA antibodies. (B) MIN6 cells were infected with recombinant adenovirus encoding either HA-tagged exophilin7 or granuphilin cDNA. Immunoprecipitates by anti-HA antibodies or control immunoglobulin G, as well as 1/75 of the original cell extract, were immunoblotted with antibodies against HA-tag, syntaxin-1a, Munc18-1, and Rab27a.

the binding activities to Munc18-1 (Coppola *et al.*, 2002) and to the Munc18-1–interacting, plasma membrane–soluble *N*-ethylmaleimide-sensitive factor attachment protein receptor syntaxin-1a (Torii *et al.*, 2002, 2004; Wang *et al.*, 2011). We thus examined the binding activity of exophilin7 to these proteins. Syntaxin-1a in solution exists in equilibrium between a fusion-incompetent, closed form and a fusion-competent, open form. To determine the form to which exophilin7 might bind, we subjected both wild-type syntaxin-1a and the mutant L165A/E166A, which is known to adopt a constantly open conformation in vitro (Dulubova *et al.*, 1999), to binding assays. HA-granuphilin translated in vitro preferentially bound wild-type syntaxin-1a compared with the open-form mutant (Figure 7A, top), as reported previously in the extract of MIN6 cells (Torii *et al.*, 2002). By contrast, HA-exophilin7 exhibited little or no binding to either form of syntaxin-1a. Furthermore, HA-exophilin7 did not bind to glutathione *S*-transferase (GST)-fused Munc18-1, in contrast to HA-granuphilin (Figure 7A, bottom). We next performed coimmunoprecipitation experiments to investigate the complex formation in intact cells. For this purpose, we separately expressed HA-granuphilin and HA-exophilin7 in MIN6 cells by recombinant adenoviruses encoding the respective proteins and then immunoprecipitated them with anti-HA antibody. Although Rab27a was found in both granuphilin- and exophilin7-immunoprecipitates, syntaxin-1a and Munc18-1 were detected only in the former immunoprecipitate (Figure 7B). Therefore exophilin7 could not form a complex with syntaxin-1a or Munc18-1 even when it was overexpressed in cells.

Phospholipid-binding activity of exophilin7 mediates its exocytic ability

Although the affinities toward the Munc18-1/syntaxin-1a complex on the plasma membrane could determine the presence or absence of the activities of the two Rab27a effectors toward stably docked granules, it remains unknown how exophilin7 tethers undocked granules to the plasma membrane transiently for fusion without an affinity to the protein complex. We previously showed that exophilin4 executes the targeting of glucagon granules to the plasma membrane primarily through the affinity of its C2A domain toward phospholipids, such as phosphatidylserine (PS) and/or phosphatidylinositol-4,5-bisphosphate (PIP_2; Yu *et al.*, 2007). Furthermore, it was previously reported that the C2A domain of JFC1, a human homologue of mouse exophilin7, preferentially binds to phosphatidylinositol 3,4,5-triphosphate (PIP_3) in vitro, localizes to the plasma membrane in the fibroblast embryonic cell line NIH 3T3, and dissociates from it in the cells treated with either phosphoinositide (PI) 3-kinase inhibitor or Ca^{2+} ionophore (Catz *et al.*, 2002), suggesting that the Ca^{2+}-inhibitory affinity of the exophilin7 C2A domain to 3′-PI is responsible for its location on the plasma membrane. Thus, in the present study, we examined the Ca^{2+}- and phospholipid-binding activity of the C2 domains of exophilin7 in comparison with those of granuphilin by liposome-binding assays (Figure 8A). Although the C2A domain of exophilin7 exhibited a binding activity to the PS and PIP_2 liposomes comparable to the C2 domains of granuphilin (Figure 8, B and C), it showed neither the preferential binding activity to PIP_3 compared with PIP_2 nor the Ca^{2+}-inhibitory phospholipid-binding activity (Figure 8, B–D), in contrast to the previous finding (Catz *et al.*, 2002). Furthermore, the strength of the PIP_3-binding activity of exophilin7 was not greater than that of granuphilin. These discrepancies may be due to differences in the assay conditions. The C2B domain of exophilin7 had no significant binding activity to any of these liposomes, consistent with the previous finding that it localizes in the cytosol when expressed in NIH 3T3 cells (Catz *et al.*, 2002). We introduced mutations into the C2A domain of exophilin7, designated KQ, which changes a cluster of four lysine and one arginine residues to glutamine residues. The corresponding mutant in the C2A domain of exophilin4 has been shown to lose both the phospholipid-binding activity in vitro and the granule-targeting activity toward the plasma membrane in pancreatic α cells (Yu *et al.*, 2007). As expected, the KQ mutant of exophilin7 lost the binding activity to the PS, PIP_2, and PIP_3 liposomes (Figure 8, B–D). However, the KQ mutant expressed in MIN6 cells remained localized on the insulin granule membrane (Supplemental Figure S4). Quantification revealed that 52.6 ± 4.8% ($n = 24$) of the KQ mutant-positive puncta contain insulin, which was similar to the value of the wild type (56.3 ± 4.2%; $n = 21$). These findings suggest that exophilin7 associates with the granules through its N-terminal Rab27-binding domain.

We next investigated whether the drastic change in the affinity to the phospholipids affects the exocytic activity of exophilin7. We expressed full-length exophilin7 protein that contained either the wild-type or KQ mutant C2A domain in pancreatic β cells from exophilin7-knockout mice and examined fusion events of fluorescently labeled insulin granules by TIRF microscopy (Figure 8E). Compared with the wild type, the KQ mutant significantly reduced the numbers of fusion events from *visitors* and *passengers*, although it also tended to decrease those from *residents* (Figure 8F). It should be noted that some *residents* may not necessarily be directly attached or molecularly docked to the plasma membrane because a considerable number of granules are still visible in granuphilin-null β cells by TIRF microscopy despite the lack of docked granules at the electron microscopic level (Kasai *et al.*, 2008). These findings suggest that the phospholipid-binding activity is indispensable for exophilin7 to recruit granules to the plasma membrane to promote their exocytosis.

DISCUSSION

In contrast to our conventional understanding, recent TIRF microscopic recordings of individual granule exocytosis in living cells at a

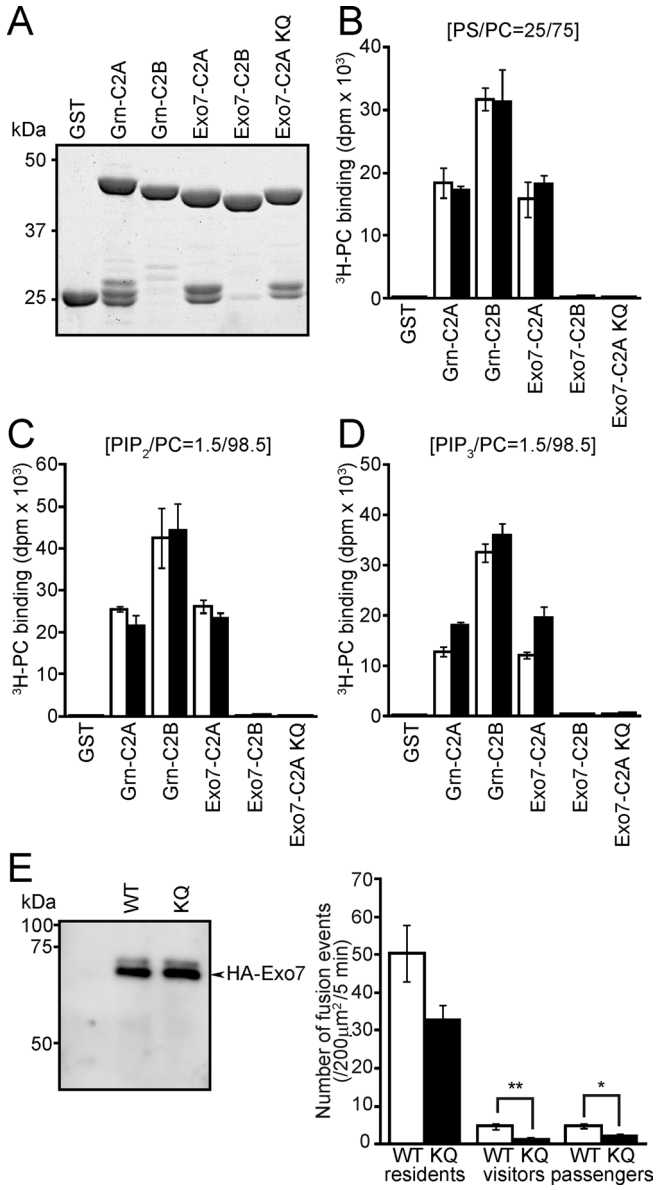

FIGURE 8: Phospholipid-binding activity is required for exophilin7-mediated exocytosis. (A–D) Liposome binding to the C2 domains of exophilin7 (Exo7) and granuphilin (Grn). (A) Equivalent amounts of each GST-fused protein were electrophoresed on a polyacrylamide gel and stained with Coomassie blue. (B–D) GST-fused recombinant proteins bound to glutathione beads were incubated with ^{3}H-labeled liposomes in the absence (open bars) or presence (solid bars) of 100 μM Ca^{2+}. The ^{3}H-labeled liposomes were composed of phosphatidylcholine mixed with either 25 wt% of PS (B), 1.5 wt% of PIP_2 (C), or 1.5 wt% of PIP_3 (D). Phospholipid binding was measured by scintillation counting of the beads after extensive washing and are represented as means ± SEM (n = 3). (E) A monolayer of β cells from exophilin7-KO mice was coinfected with adenovirus encoding EGFP-tagged human preproinsulin (moi 28) and with that encoding HA-tagged, WT or KQ mutant exophilin7 (moi 25). After 2 d, expression levels of HA-tagged exogenous exophilin7 were determined by immunoprecipitation, followed by immunoblotting with anti-HA antibodies (left), or high potassium-induced fusion events were analyzed by TIRF microscopy as in Figure 5 (right). The number of fusion events during the stimulation is summed for each category of granules in WT (open columns) and KQ mutant (closed columns) exophilin7-expressing cells. Data are expressed as the mean ± SEM (n = 10). The statistical significance of differences between means was assessed by a Mann–Whitney U test. *$p < 0.05$; **$p < 0.005$.

very short interval (50–300 ms) revealed heterogeneous prefusion steps among fused granules and demonstrated that stable docking is not a necessary first step before a granule can acquire fusion competence (priming; Ohara-Imaizumi *et al.*, 2004; Shibasaki *et al.*, 2007; Kasai *et al.*, 2008; Izumi, 2011). Moreover, observations of granuphilin-null β cells revealed that stable docking may even be inhibitory for subsequent fusion (Gomi *et al.*, 2005; Izumi *et al.*, 2007; Kasai *et al.*, 2008). These findings indicate that undocked granules can efficiently undergo exocytosis, although the molecular mechanism of undocked granule exocytosis is largely unknown. In the present study, we showed that the Rab27a effector exophilin7 mediates the exocytosis of undocked granules, based on the following findings. First, exophilin7 overexpressed in MIN6 cells does not stably target or accumulate granules near the plasma membrane, in contrast to another Rab27a effector, granuphilin (Torii *et al.*, 2004). Second, exophilin7-null β cells exhibit impairment of depolarization-induced exocytosis especially from a *passenger* type of granule, which fuses without stable visualization before fusion under TIRF microscopy and thus is believed to fuse without stably docking to, or stalling near, the plasma membrane. Finally, and most convincingly, exophilin7 deficiency affects evoked granule exocytosis in the absence of any stably docked granules, which is caused by a simultaneous granuphilin deficiency. The present report is the first to identify exophilin7 as a molecule that functions in the exocytosis of undocked granules, and this finding elucidates, at least in part, the molecular basis for the *passenger* type of exocytosis. Therefore granuphilin and exophilin7, the two Rab27a effectors coexpressed in β cells, differentially mediate the exocytosis of docked and undocked granules, respectively.

To explore the underlying mechanism for the functional differences between the two Rab27 effectors, we compared their biochemical properties. The phospholipid-binding activity of exophilin7 C2A domain was not much different from that of granuphilin. Furthermore, although the C2B domain of exophilin7 showed a negligible binding activity to the plasma membrane phospholipids compared with that of granuphilin, it could not account for the absence of granule-targeting activity in exophilin7, considering that the granuphilin-b isoform lacking its C2B domain has a stronger granule-targeting activity than does the granuphilin-a isoform containing both C2 domains (Torii *et al.*, 2004). However, there are clear differences between the protein interactions of exophilin7 and granuphilin: only granuphilin interacts with a fusion-inhibitory Munc18-1/syntaxin-1a complex. These findings suggest that the affinities to these proteins may determine the presence or absence of the activities of the two Rab27a effectors to stably dock granules to the plasma membrane and to inhibit their fusion. Consistent with this idea, it has been shown that Munc18-1–null chromaffin cells exhibit a granule-docking defect (Voets *et al.*, 2001). However, it is unknown how exophilin7 mobilizes undocked granules near the plasma membrane for fusion without an affinity to the protein complex. It was previously shown that another Rab27a effector, exophilin4, targets glucagon granules to the plasma membrane through the affinity of its C2A domain toward phospholipids such as PS and/or PIP_2 (Yu *et al.*, 2007). We also found that the C2A domain of granuphilin is essential for its granule-targeting activity (unpublished data), although it is not involved in the interaction with the Munc18-1/syntaxin-1a complex (Torii *et al.*, 2002; Tsuboi and Fukuda, 2006). In the present study, the rescue expression of the exophilin7 KQ mutant lacking the phospholipid-binding activity in its C2A domain in exophilin7-null β cells induced a lower number of fusion events from incoming undocked granules compared with that of wild-type exophilin7, suggesting that this activity is instrumental in recruiting them

to the plasma membrane. Taken together, those C2 domain-containing Rab27 effectors appear to tether granules to the plasma membrane through the phospholipid-binding activity of its C2A domain, although the exact nature of the target phospholipid is unknown.

In summary, we demonstrated that the Rab27a effector exophilin7 actively mediates the exocytosis of undocked granules. However, other mechanisms must also be involved in this process because fusion from undocked granules is only partially impaired in exophilin7-null cells. Nevertheless, these findings represent the first documentation that docked and undocked granules fuse in parallel, but not in sequence, using distinct Rab27 effectors expressed in the same secretory cell, as was suggested previously (Izumi *et al.*, 2007).

MATERIALS AND METHODS

DNA construction

Full-length exophilin7 cDNA amplified from the cDNA of the MIN6 mouse pancreatic β-cell line by PCR was subcloned into the pcDNA3-HA to express HA-tagged protein. Recombinant adenoviruses bearing HA-tagged exophilin7 and granuphilin cDNAs were prepared as described previously (Yi *et al.*, 2002). Site-directed mutagenesis of exophilin7 was performed by using the following primers: 5′-GGGGAATTCATGCCCCAGAGAGGCCAC-3′ and 5′- CACACTAGTCTGTTGCTGGCTCTGCTTATCCGGGAGG-3′ for KQ1 and 5′-AAGACTAGTGTGCAGCAACGGAATCTGAACCCGATC-3′ and 5′-GGGCTCGAGCTATGCCCTGGGGACCAG-3′ for KQ2. The KQ mutant was constructed by ligating the cDNA fragments containing the respective KQ1 and KQ2 mutations. The resulting exophilin7-C2A^{KQ} carries substitutions of glutamine for lysine or arginine at amino acid positions 322, 323, 324, 328, and 329. To generate GST-fused proteins, mouse Munc18-1 cDNA was subcloned into the pGEX-KG (Guan and Dixon, 1991), and the cDNA fragments encoding 1–282 (N-terminal domain), 270–386 (C2A domain), and 421–545 (C2B domain) amino acids of exophilin7 were subcloned into the pGEX4T-1 (GE Healthcare, Piscataway, NJ). The GST-fused cDNA construct containing granuphilin C2A or C2B domain was described previously (Wang *et al.*, 1999).

Antibodies, immunoblotting, immunoprecipitation, and immunostaining

Rabbit anti-exophilin7 antibody (αExo7N) was raised against GST-fused N-terminal exophilin7 protein. The sera were passed through a column containing GST protein, followed by one containing GST-fused N-terminal exophilin7 protein. The affinity-purified antibodies were then eluted and concentrated. The preparation of anti-granuphilin antibody (αGrp-N) was described previously (Yi *et al.*, 2002). Mouse anti-Rab27a and anti–Munc18-1 monoclonal antibodies were purchased from BD Bioscience Transduction Laboratories (Lexington, KY). Mouse anti–syntaxin-1 (HPC-1) and anti–α-tubluin monoclonal antibodies were purchased from Sigma-Aldrich (St. Louis, MO). Mouse anti-synaptophysin monoclonal antibody was purchased from Progen Biotechnik (Heidelberg, Germany). Rat anti-HA (clone 3F10) monoclonal antibody was purchased from Roche Diagnostics (Mannheim, Germany). Guinea pig anti–porcine insulin serum was a gift from H. Kobayashi (Gunma University, Maebashi, Japan).

MIN6 cells and HEK293A cells were grown in high-glucose (25 mM) DMEM supplemented with 15% fetal calf serum and 55 μM 2-mercaptoethanol and with 10% fetal calf serum, respectively. Tissue extract preparation and subcellular fractionation on a linear sucrose density gradient for immunoblotting analysis were performed as described previously (Yi *et al.*, 2002; Hosaka *et al.*, 2007). Plasmid transfections and adenovirus infections were performed as described previously (Yu *et al.*, 2007). Immunoblotting, immunoprecipitation, and in vitro binding with GST fusion protein were also performed as described previously (Wang *et al.*, 2011). Indirect immunofluorescence analyses were performed with a confocal microscope as described previously (Yu *et al.*, 2007). Colocalization was quantified with the RG2B colocalization plug-in of ImageJ software (National Institutes of Health, Bethesda, MD).

Plasma membrane targeting and insulin secretion assays in MIN6 cells

A targeting assay was performed as described previously (Torii *et al.*, 2004), with minor modification. Briefly, MIN6 cells stably expressing phogrin-EGFP were seeded at 1×10^5 cells in an eight-well chamber. The cells were infected with a recombinant adenovirus encoding β-galactosidase (β-gal), HA-exophilin7, or HA-granuphilin cDNA. After 24 h, the cells were processed for indirect immunofluorescence analysis. Intrinsic EGFP and antibody staining signals were observed by confocal microscopy. A peripheral pattern of EGFP signals was quantified as described previously (Yu *et al.*, 2007): cells that revealed a linear distribution along 76–100% of the whole plasma membrane were counted as 1, those along 51–75% as 0.75, those along 26–50% as 0.5, those along <25% as 0.25, and those that showed no linear distribution as 0. The summed counts divided by the number of cells examined was defined as the targeting activity. The effect of overexpressed exophilin7 or granuphilin on insulin secretion in MIN6 cells was examined as described previously (Yi *et al.*, 2002). Insulin secreted in the buffer was measured in duplicate by a radioimmunoassay (Eiken Chemical, Tokyo, Japan).

Generation of exophilin7-deficient mice

The genomic DNA clone encoding mouse exophilin7 (*Sytl-1*) in a C57BL/6J BAC genomic library (RPCI-23.C) was purchased from Invitrogen (clone ID: 233N12; Carlsbad, CA). The targeting vector p5′EX-*pgk-neo*-3′NH-*DTA* was constructed with a 6.2-kb *Eco*RI–*Xba*I fragment that spans from 5′ untranslated region to exon 1 as a 5′ homologous region, a 3.9-kb *Nco*I–*Hin*dIII fragment from exon 2 to intron 8 as a 3′ homologous region, a 2.1-kb floxed *pgk-neo* fragment in which a *pgk-neo* gene (a gift from M. A. Rudnicki, Ottawa Health Research Institute, Ottawa, Canada) is flanked by two *loxP* sequences, and a 1.4-kb diphtheria toxin A–fragment gene cassette derived from p*MC1DTA-pA* (a gift from T. Yagi, Osaka University, Suita, Japan; Yanagawa *et al.*, 1999). The targeting vector was electroporated into BA1 (129SvEv × C57BL/6 hybrid) embryonic stem cells, and G418-resistant clones were selected. Homologous recombinants were screened by PCR and Southern blot hybridization. The primers designed for the 5′ PCR were *5′SacI/Fow*, 5′-CTCAGGAGCTCCGCTCTTCCCTCCAGA-3′; and *3′neo1FR/Rev*, 5′-CAGGAGCAAGGTGAGATGACAGGAGATCCT-3′; and those for the 3′ PCR were *5′neofow2/Fow*, 5′-CTTGACGAGTTCTTCTGAGG-3′; and *3′exon9/Rev*, 5′-CCCTGTTCATTTGCAGGGATGACAG-3′. For Southern blot hybridization, the genomic DNA digested with *Sac*I or *Kpn*I was hybridized with an alkaline phosphatase–labeled (AlkPhos Direct; GE Healthcare) 939–base pair *Sac*I/*Eco*RI fragment as a 5′ external probe or with a 634–base pair *Hin*dIII/*Kpn*I fragment as a 3′ external probe, using a GeneScreen Plus Hybridization Transfer Membrane (PerkinElmer, Wellesley, MA). The embryonic stem cell clones containing the targeting event were microinjected into C57BL/6J blastocysts to generate chimeric mice. The mice heterozygous for the targeted allele were obtained by crossing the male chimeras with female C3H/He mice. Mutant lines were backcrossed

with C3H/He mice for 5–10 generations. Genotype analysis was done by PCR using the primers designed for the exon 2 region of *Sytl-1* and *pgk-neo*: *Exo7/Fow2*, 5′-CAGCTGATGCCCCAGAGAGGC-3′; *Exo7/Rev*, 5′-TCTCGTTTGAGGACATCAGAGATG-3′; and *neofow2/Fow*, 5′-CTTGACGAGTTCTTCTGAGG-3′. Exophilin7/granuphilin double-knockout mice were obtained by mating the exophilin7-knockout mice with the granuphilin-knockout mice (Gomi *et al.*, 2005).

Phenotypic analyses of mice

All animal experiments were performed in accordance with the rules and regulations of the Animal Care and Experimentation Committee, Gunma University, Japan. Mice had free access to water and standard laboratory chow in an air-conditioned room with a 12-h light/12-h dark cycle. An intraperitoneal glucose tolerance test (1 g glucose/kg body weight) and an intraperitoneal insulin tolerance test (0.75 U human insulin/kg body weight) were performed as described previously (Wang *et al.*, 2011). Blood glucose levels were determined by a glucose oxidase method using Glutest sensor and Glutest Pro GT-1660 (Sanwa Kagaku Kenkyujyo, Nagoya, Japan). The serum insulin concentration was measured by an LBIS mouse insulin enzyme-linked immunosorbent assay kit (U-type; Shibayagi, Shibukawa, Japan). Islet isolation by pancreatic duct injection of collagenase solution and insulin secretion assay in perifused islets were performed as described previously (Wang *et al.*, 2011). Insulin was measured using an AlphaLISA insulin kit with an EnVision 2101 Multilabel Reader (PerkinElmer). The examination of granule distribution by electron microscopy was performed as described previously (Gomi *et al.*, 2005). Measurement of the concentration of cytoplasmic free Ca^{2+} was performed as described previously (Mizuno *et al.*, 2011).

TIRF microscopic analysis of exocytosis of insulin granules

A monolayer of primary mouse β cells was infected with adenovirus encoding EGFP-tagged human preproinsulin and further cultured for 2 d. Before image recording by TIRF microscopy, the cells were incubated for 30 min in standard Krebs–Ringer buffer at 37°C. TIRF microscopy was performed using an inverted microscope (Eclipse; Nikon, Tokyo, Japan) with a 1.49–numerical aperture objective (Apo TIRF 100×; Nikon). The penetration depth of the evanescent field (160 nm) was calculated as described previously (Axelrod, 2001). Images were acquired at 101.7-ms intervals with an electron-multiplying charge-coupled device camera (iXon DU-897; Andor Technology, Belfast, Northern Ireland) controlled by NIS-element software (Nikon). Under TIRF microscopy, the cells were incubated with standard Krebs–Ringer buffer for the first 30 s and then exposed to high-potassium stimulation for 5 min. Stimulation was achieved by the addition of the same volume of twofold concentrated solution, resulting in a final concentration of 60 mM potassium. Fusion events with a flash were manually selected and assigned to one of three categories: *residents*, which are visible before stimulation; *visitors*, which have become visible during stimulation and remained visible for >101.7 ms (the interval of one frame) before fusion; and *passengers*, which are visible for <101.7 ms before fusion, as described previously (Kasai *et al.*, 2008). The average fluorescence intensity of individual vesicles was calculated in a 0.7 μm × 0.7 μm square around the vesicle by NIS-element software.

Phospholipid-binding assays

Bacterially expressed GST-fused proteins were affinity purified with glutathione–Sepharose 4B beads. The phospholipid-binding assays were performed as described previously (Yu *et al.*, 2007). All phospholipids were purchased from Avanti Polar Lipids (Alabaster, AL).

ACKNOWLEDGMENTS

We are grateful to S. Torii for molecular cloning of exophilin7 cDNA, T. Nara and T. Ushigome for their colony management of mice, and J. Toshima for her assistance in preparing the manuscript. This work was supported by grants-in-aid for scientific research (to R. I. and T. I.) and a grant of the Global COE Program from the Ministry of Education, Culture, Sports, Science and Technology of Japan. It was also supported by grants from the Mitsubishi Foundation and by a Novo Nordisk Insulin Study Award (to T. I.).

REFERENCES

Axelrod D (2001). Total internal reflection fluorescence microscopy in cell biology. Traffic 2, 764–774.

Brzezinska AA, Johnson JL, Munafo DB, Crozat K, Beutler B, Kiosses WB, Ellis BA, Catz SD (2008). The Rab27a effectors JFC1/Slp1 and Munc13-4 regulate exocytosis of neutrophil granules. Traffic 9, 2151–2164.

Catz SD, Johnson JL, Babior BM (2002). The C2A domain of JFC1 binds to 3′-phosphorylated phosphoinositides and directs plasma membrane association in living cells. Proc Natl Acad Sci USA 99, 11652–11657.

Coppola T, Fantz C, Perret-Menoud V, Gattesco S, Hirling H, Regazzi R (2002). Pancreaticβ-cell protein granuphilin binds Rab3 and Munc-18 and controls exocytosis. Mol Biol Cell 13, 1906–1915.

Dulubova I, Sugita S, Hill S, Hosaka M, Fernandez I, Südhof TC, Rizo J (1999). A conformational switch in syntaxin during exocytosis: role of munc18. EMBO J 18, 4372–4382.

Fukuda M (2005). Versatile role of Rab27 in membrane trafficking: focus on the Rab27 effector families. J Biochem 137, 9–16.

Gomi H, Mizutani S, Kasai K, Itohara S, Izumi T (2005). Granuphilin molecularly docks insulin granules to the fusion machinery. J Cell Biol 171, 99–109.

Gomi H, Mori K, Itohara S, Izumi T (2007). Rab27b is expressed in a wide range of exocytic cells and involved in the delivery of secretory granules near the plasma membrane. Mol Biol Cell 18, 4377–4386.

Guan K, Dixon JE (1991). Eukaryotic proteins expressed in *Escherichia coli:* an improved thrombin cleavage and purification procedure of fusion proteins with glutathione *S*-transferase. Anal Biochem 192, 262–267.

Hannah MJ, Hume AN, Arribas M, Williams R, Hewlett LJ, Seabra MC, Cutler DF (2003). Weibel-Palade bodies recruit Rab27 by a content-driven, maturation-dependent mechanism that is independent of cell type. J Cell Sci 116, 3939–3948.

Hosaka M, Watanabe T, Yamauchi Y, Sakai Y, Suda M, Mizutani S, Takeuchi T, Isobe T, Izumi T (2007). A subset of p23 localized on secretory granules in the pancreaticβ-cells. J Histochem Cytochem 55, 235–245.

Izumi T (2011). Heterogeneous modes of insulin granule exocytosis: molecular determinants. Front Biosci 16, 360–367.

Izumi T, Gomi H, Kasai K, Mizutani S, Torii S (2003). The roles of Rab27 and its effectors in the regulated secretory pathways. Cell Struct Funct 28, 465–474.

Izumi T, Kasai K, Gomi H (2007). Secretory vesicle docking to the plasma membrane: molecular mechanism and functional significance. Diabetes Obes Metab 9, Suppl 2, 109–117.

Johnson JL, Ellis BA, Noack D, Seabra MC, Catz SD (2005). The Rab27a-binding protein, JFC1, regulates androgen-dependent secretion of prostate-specific antigen and prostatic-specific acid phosphatase. Biochem J 391, 699–710.

Kasai K, Fujita T, Gomi H, Izumi T (2008). Docking is not a prerequisite but a temporal constraint for fusion of secretory granules. Traffic 9, 1191–1203.

Kasai K, Ohara-Imaizumi M, Takahashi N, Mizutani S, Zhao S, Kikuta T, Kasai H, Nagamatsu S, Gomi H, Izumi T (2005). Rab27a mediates the tight docking of insulin granules onto the plasma membrane during glucose stimulation. J Clin Invest 115, 388–396.

Matsumoto M *et al.* (2004). Noc2 is essential in normal regulation of exocytosis in endocrine and exocrine cells. Proc Natl Acad Sci USA 101, 8313–8318.

Mizuno K, Ramalho JS, Izumi T (2011). Exophilin8 transiently clusters insulin granules at the actin-rich cell cortex prior to exocytosis. Mol Biol Cell 22, 1716–1726.

Ohara-Imaizumi M, Nishiwaki C, Kikuta T, Nagai S, Nakamichi Y, Nagamatsu S (2004). TIRF imaging of docking and fusion of single insulin granule motion in primary rat pancreatic β-cells: different behaviour of granule motion between normal and Goto-Kakizaki diabetic rat β-cells. Biochem J 381, 13–18.

Saegusa C, Kanno E, Itohara S, Fukuda M (2008). Expression of Rab27B-binding protein Slp1 in pancreatic acinar cells and its involvement in amylase secretion. Arch Biochem Biophys 475, 87–92.

Shibasaki T *et al*. (2007). Essential role of Epac2/Rap1 signaling in regulation of insulin granule dynamics by cAMP. Proc Natl Acad Sci USA 104, 19333–19338.

Tolmachova T, Anders R, Stinchcombe J, Bossi G, Griffiths GM, Huxley C, Seabra MC (2004). A general role for Rab27a in secretory cells. Mol Biol Cell 15, 332–344.

Torii S, Takeuchi T, Nagamatsu S, Izumi T (2004). Rab27 effector granuphilin promotes the plasma membrane targeting of insulin granules via interaction with syntaxin 1a. J Biol Chem 279, 22532–22538.

Torii S, Zhao S, Yi Z, Takeuchi T, Izumi T (2002). Granuphilin modulates the exocytosis of secretory granules through interaction with syntaxin 1a. Mol Cell Biol 22, 5518–5526.

Tsuboi T, Fukuda M (2006). The Slp4-a linker domain controls exocytosis through interaction with Munc18-1.syntaxin-1a complex. Mol Biol Cell 17, 2101–2112.

Voets T, Toonen RF, Brian EC, de Wit H, Moser T, Rettig J, Südhof TC, Neher E, Verhage M (2001). Munc18-1 promotes large dense-core vesicle docking. Neuron 31, 581–591.

Wang H, Ishizaki R, Kobayashi E, Fujiwara T, Akagawa K, Izumi T (2011). Loss of granuphilin and loss of syntaxin-1A cause differential effects on insulin granule docking and fusion. J Biol Chem 286, 32244–32250.

Wang J, Takeuchi T, Yokota H, Izumi T (1999). Novel rabphilin3-like protein associates with insulin-containing granules in pancreatic beta cells. J Biol Chem 274, 28542–28548.

Waselle L, Coppola T, Fukuda M, Iezzi M, El-Amraoui A, Petit C, Regazzi R (2003). Involvement of the Rab27 binding protein Slac2c/MyRIP in insulin exocytosis. Mol Biol Cell 14, 4103–4113.

Yanagawa Y, Kobayashi T, Ohnishi M, Kobayashi T, Tamura S, Tsuzuki T, Sanbo M, Yagi T, Tashiro F, Miyazaki J (1999). Enrichment and efficient screening of ES cells containing a targeted mutation: the use of DT-A gene with the polyadenylation signal as a negative selection maker. Transgenic Res 8, 215–221.

Yi Z, Yokota H, Torii S, Aoki T, Hosaka M, Zhao S, Takata K, Takeuchi T, Izumi T (2002). The Rab27a/granuphilin complex regulates the exocytosis of insulin-containing dense-core granules. Mol Cell Biol 22, 1858–1867.

Yu M, Kasai K, Nagashima K, Torii S, Yokota-Hashimoto H, Okamoto K, Takeuchi T, Gomi H, Izumi T (2007). Exophilin4/Slp2-a targets glucagon granules to the plasma membrane through unique Ca^{2+}-inhibitory phospholipid-binding activity of the C2A domain. Mol Biol Cell 18, 688–696.